Magazine of Civil Engineering. 2019. 88(4). Pp. 70–79
Инженерно-строительныйжурнал. 2019. № 4(88). С. 70–79

Magazine of Civil Engineering

ISSN 2071-0305

journal homepage: http://engstroy.spbstu.ru/

DOI: 10.18720/MCE.88.7

Reducing temperature difference in mass concrete by surface insulation

T.C. Nguyen[a]*, X.B. Luu[b]
[a]Moscow State University of Civil Engineering, Moscow, Russia
[b]Tri Dung Construction Transportation Joint Stock Company, Dong Nai, Vietnam
** E-mail: ntchuc.mta198@gmail.com*

Keywords: heat of hydration, temperature gradient, crack, mass concrete, mathematical model, sand-layer insulation.

Abstract. The heat which is produced in the cement hydration is rather high in mass concrete structures like dams, pavements, piers. In fact, it takes a longer time to cool the inner of the mass than its surface. The main reason for this result is that having the temperature difference between the hot inner mass and its cooled surface. Such a gap like that is the cause of appearing a large number of cracks in the surface of the mass concrete at several days age. In this study, the application of using a sand-layer insulation to control mass concrete block cracks at an early age. Specifically, these processes are performed by the program Midas Civil 2017 in cases: without sand-layer insulation, and with the application of using sand-layer insulation have thickness in range of 0–7 cm for heat preservation. In conclusion, the results in this study showed that when using an insulation thickness of 7 cm, it led to that the maximum temperature differences between the surface and the center of mass concrete block is lower than the limitation. The recommendations made as a result of this study is that sand-layer insulation should be used to prevent and limit cracks of the mass concrete block at an early age.

1. Introduction

The increase in temperature during concrete hardening is due to the exothermic hydration reactions of water and cement. This is important for massive elements, in which conditions are close to adiabatic temperature can reach in range of 50÷90 °C has been described by ACI Committee [1–3]. The cause affecting the high-temperature rise and its non-uniform distribution between the surface and inside of thick slabs is low thermal conductivity of concrete, which slows down the natural cooling process. In the meantime, the shrinkage deformations are formed during the hydration of concrete as a result of a chemical reaction and the moisture exchange with the environment. According to published study, the result is on the surface of the concrete block in all the cracks [4–6].

There is a variety of methods and different prices to control the temperature of mass concrete such as low-heat materials, pre-cooling of concrete, posts-cooling of concrete. Each method has its advances depend on specific situations [7–9].

Surface heat preservation is an important measure for temperature control and cracks prevention. Many types of insulation materials are available in the world today, and insulation levels can be optimized to meet the required temperature differences in mass concrete. The selection of insulation material types and thicknesses are particularly important. So, based on that information can reduce the difference in temperature between the center and the surface of the concrete block by applying the insulation layer on the surface of the raft foundation, as can be seen in Figure 1.

Nguyen, T.C., Luu, X.B. Reducing temperature difference in mass concrete by surface insulation. Magazine of Civil Engineering. 2019. 88(4). Pp. 70–79. DOI: 10.18720/MCE.88.7

Нгуен Ч.Ч., Лыу С.Б. Уменьшение разницы температур в монолитном бетоне за счет поверхностной изоляции // Инженерно-строительный журнал. 2019. № 4(88). С. 70–79. DOI: 10.18720/MCE.88.7

Figure 1. Different types of insulation materials of the surface [10].

Thermal insulation is often used to warm the concrete surface and reduce the temperature difference, which in turn minimizes the thermal cracking ability. The surface insulation can significantly reduce the cooling rate while its effect on the maximum concrete temperature is not considered in most of the mass concrete pours. Insulation is inexpensive, but the result may be delayed due to by reducing the cooling rate, which can be costly. It is necessary to maintain the insulation for several weeks or longer because its surface could be cooled quickly and cracked when removing it too early. There are many types of insulation materials and its usage can be optimized to adapt to the requirement of temperature differences and maximize the cooling rate has been described by [11–12]. The small and medium-sized projects could also use straw bags and sand layers as insulation. The control of the thickness of the sand layer is conducted to determining the volume ratio on the sand was transported to the surface area of concrete blocks. However, with the structure has an inclined or vertical surface, the use of insulating sand layer is not effective, but in this situation could use polystyrene slab instead of sand insulation. The optimal time of putting or removing the sand layer on the block surfaces should be carefully considered based on the rate of strength development in concrete and the processing of heat of cement hydration. With high wind or heavy rain conditions, shielding methods must be taken to avoid sand erosion as well as undesirable sand thickness changes. Besides that, in order to collect of sand after use on the surface of the concrete is convenient should putting a layer of tarpaulin (or nylon) in advance, then spreading a sand layer on the tarpaulin.

The goal of this paper is to study the application of using sand-layer insulation to control mass concrete block cracks at an early age by finite element method using Midas Civil software 2017. The results show that using sand-layer insulation can considerably reduce maximum tensile stress.

2. Materials and methods

The study of the temperature regime of massive concrete blocks has been devoted to a rather large number of works carried out using modern methods. In this paper, applications by an insulating layer of sand to control the cracks of massive concrete blocks at the age of early days by finite element method using the software Midas civil 2017.

The solution to the temperature problem is based on the solution of the differential equation of the theory of heat conduction can be expressed as [13–16].

$$\frac{\partial}{\partial x}\left(k_x\frac{\partial t}{\partial x}\right)+\frac{\partial}{\partial y}\left(k_y\frac{\partial t}{\partial y}\right)+\frac{\partial}{\partial z}\left(k_z\frac{\partial t}{\partial z}\right)+q_v=\rho c\frac{\partial t}{\partial \tau}, \quad (1)$$

where t is the material temperature (°C);

k_x, k_y, k_z are the thermal conductivity coefficients of the material dependent on the temperature in the directions x, y and z, respectively; (W/m.°C);

q_v is the amount of heat released by internal sources (for example, exothermic heating) to a given moment in time (W/m^3);

c is specific heat (kJ/kg.°C);

ρ is the density concrete (kg/m^3);

τ is time (day).

Four types of boundary conditions are used to the solution of problems of heat transfer equation (1) as Dirichlet boundary conditions, Neumann boundary conditions, Robin boundary conditions, and Nonlinear, mixed boundary conditions [17].

The solution of problems for determining the temperature regime and the thermally stressed state of concrete massive structures today often obtained using numerical methods (most often the finite element method (FEM)). The value of the temperature of a function at any point in the computational domain in the finite element method is expressed in terms of time and coordinates [18–19].

$$t(x,y,z,\tau) \approx \bar{t} = \sum_{i=1}^{n} N_i(x,y,z) t_i(\tau) = \left[N\right]\left\{t\right\}, \tag{2}$$

where N_i is the interpolation function of the shape of the finite element with respect to temperature and coordinates;

n is the number of points in the final element;

$t_i\ (\tau)$ is the temperature at each point as a function of time.

In accordance with the Galerkin method, equation (1) is described:

$$\begin{aligned} &\int_V N_i \left[\frac{\partial}{\partial x}\left(k_x \frac{\partial t}{\partial x}\right) + \frac{\partial}{\partial y}\left(k_y \frac{\partial t}{\partial y}\right) + \frac{\partial}{\partial z}\left(k_z \frac{\partial t}{\partial z}\right)\right] dV \left\{t\right\} + \int_S h\left[N\right] N_i \left\{t\right\} dS - \\ &-\int_S h N_i t_\infty dS + \int_S q N_i dS - \int_V G N_i g V + \int_V \rho C \left[N\right] N_i dV \frac{d\left\{t\right\}}{d\tau} = 0, \end{aligned} \tag{3}$$

where h is the heat transfer coefficient(W/m^2.°C);

V is volume of element (m^3);

S is the boundary conditions on surface;

q is the heat flux (W/m^3);

G is heat generation within an element (W).

We introduce the notation:

$$\begin{gathered} \left[K\right] = \int_V N_i \left[\frac{\partial}{\partial x}\left(k_x \frac{\partial t}{\partial x}\right) + \frac{\partial}{\partial y}\left(k_y \frac{\partial t}{\partial y}\right) + \frac{\partial}{\partial z}\left(k_z \frac{\partial t}{\partial z}\right)\right] dV + \int_S h\left[N\right] N_i dS \\ \left[C\right] = \int_V \rho c \left[N\right] N_i dV,\ \left[f\right] = \int_S h N_i t_\infty dS - \int_S q N_i dS + \int_V G N_i g V, \end{gathered} \tag{4}$$

where $[K]$ is conductivity operator;

$[C]$ is capacity operator;

$[f]$ is heat load due to heat hydration.

Then, by introducing equation (4) into equation (3), can be obtained equation (5) as:

$$\left[C\right]\frac{d\left\{t\right\}}{d\tau} + \left[K\right]\left\{t\right\} = \left\{f\right\}, \tag{5}$$

Applying the method of Galerkin for $t(\tau) = t_i(\tau)N_i + t_j(\tau)N_j$ each element, $N_i = 1 - \frac{\tau}{\Delta\tau}; N_j = \frac{\tau}{\Delta\tau}$. At each step, the equation is solved for the time:

$$\left(-\frac{\left[C\right]}{2\Delta t} + \frac{\left[K\right]}{3}\right)\left\{t\right\}_{(n-1)\tau} + \frac{2\left[K\right]}{3}\left\{t\right\}_{n\tau} + \left(\frac{\left[C\right]}{2\Delta t} + \frac{\left[K\right]}{6}\right)\left\{t\right\}_{(n+1)\tau} = \left\{f\right\}, \tag{6}$$

As a result, the solution of equation (6) we obtain the desired temperature field.

To illustrate the process of simulation, a flowchart of the analysis process is shown in Figure 2.

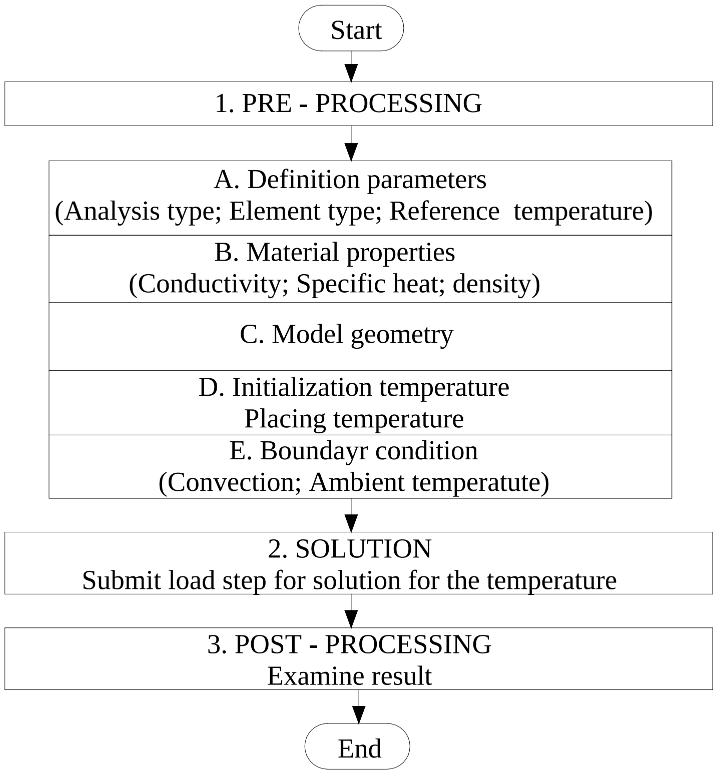

Figure 2. Process analysis of temperature fields, stress in mass concrete block by FEM.

According to the results of studies [20], the ratio between the thermal-stress and temperature in concrete mass is determined by equation (7):

$$\sigma = R \times E(\tau) \times \alpha \times \Delta T, \quad (7)$$

where σ is thermal-stresses (MPa);

R is restraint ($0 < R < 1$), the restraint coefficient which is dependent on the size of the concrete mass and the ratio of elastic module of concrete and foundation: $R \in f(V; E_c/E_f)$ and can be calculated using the computer program Midas Civil;

α is coefficient of thermal expansion (1/°C);

$E(\tau)$ is concrete elasticity modulus (MPa);

ΔT is temperature drop (°C).

The modulus of elasticity $E(\tau)$ of concrete is depend on the age τ, as described by equation (8) [21]:

$$E(\tau) = E_0(1 - e^{-a\tau^b}), \quad (8)$$

where E_0 is concrete elasticity modulus at 28 days age (N/mm^2);

a, b are determined by experiment, $a = 0.4$; $b = 0.34$ [21].

Data for example, according to standards ACI 209.2R-08 “Guide for Modeling and Calculating Shrinkage and Creep in Hardened Concrete». A creep coefficient and an unrestrained shrinkage strain at any time depend on [22]:

– Age of concrete when drying starts, usually taken as the age at the end of moist curing (days);

– Age of concrete at loading (days);

– Curing method;

– Ambient relative humidity expressed as a decimal;

– Volume-surface ratio or average thickness (m);

– Concrete slump (m);

– Fine aggregate percentage (%);

– Cement content (kg/m^3);

– Air content of the concrete expressed in percent (%); and

– Cement type.

With the help of software Midas Civil to declare parameters needed to mention creep of concrete at early age days. The creep of mass concrete may be expressed by the following formula (9).

$$J(t,\tau) = \frac{1+\varphi(t,\tau)}{E(\tau)}, \tag{9}$$

where $J(t,\tau)$ is the creep compliance whose dimension (MPa^{-1});

$\varphi(t,\tau)$ is the coefficient of creep and is equal to the ratio of creep to elastic strain is shown in Figure 3.

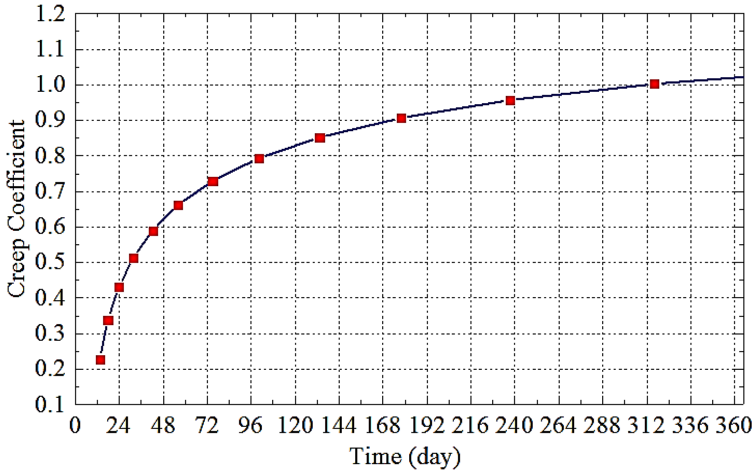

Figure 3. The coefficient of creep at different ages.

Currently, there are many ways to assess the possibility of cracking of mass concrete at an early age. In Russia, in accordance with Russian Construction Norms SP 357.1325800.2017"Concrete hydraulic structures. Rules of works and acceptance of works" [23], the temperature difference at the center and the outer surface of concrete mass ΔT is allowed no more than (20–25) °C. To describe in more detail the temperature regime of the concrete mass are established on the basis of calculations of temperature fields and the thermal stress state of the concrete mass during construction.

Besides, when the calculated principal tensile stresses exceed the tensile strength of the concrete, cracking is likely to have occurred, which can be assessed by cracking index as described by equation (10) [24].

$$I_{ct} = \frac{f_t(\tau)}{\sigma_t(\tau)}, \tag{10}$$

where I_{ct} is cracking index;

$f_t(\tau)$ is tensile strength;

$\sigma_1(\tau)$ is principal tensile stress.

If $I_{ct} \leq 1$ cracking may occur, and $I_{ct} > 1$ no cracks were formed on the concrete surface.

In this paper, numerical studies of the temperature regime of the mass concrete structure was a pier footing size 6×8×3 m that was placed in the summer weather conditions in Vietnam. There are made and studied the effect of sand layer thickness to control cracked concrete surface. The symmetry of the investigated array was used: a quarter of the concrete block was calculated. The dimensions and the breakdown of the calculation area into the final elements is shown in Figure 4.

The ambient temperature significantly effects on the maximum temperature at the center of the concrete block during the hardening process. This a mass concrete is built with air temperatures are assumed constant at 28.5 °C, soil temperature is assumed constant at 20 °C and temperature of placed concrete at 30 °C. The mix proportion is shown in Table 1 [25].

a)

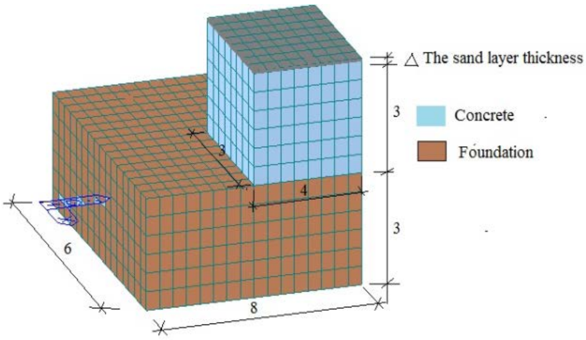

b)

Figure 4. a-A bridge pier footing constructed in Vietnam; b – 3D model for temperature analysis with an insulation layer of sand, unit m.

Table 1. Mix design of concrete.

Concrete	Ratio Water/ Cement	Materials for 1 m^3 of concrete				
		Cement (kg)	Sand (kg)	Stone (kg)	Water (l)	Additives (super flexible)
	37.5 %	445	829	1007	167	(5.12)1.15 %

The concrete adiabatic temperature is varied by introducing different cement contents. The adiabatic temperature is given by equation (11) [26].

$$t = K(1 - e^{-\alpha\tau}), \tag{11}$$

where t is the adiabatic temperature rise at age τ (°C);

K is the maximum amount of the adiabatic temperature rise from test (°C), K = 59.6 °C [26];

α is the reaction factor (°C/h), α = 1.113 [26].

Thermal insulators are meant to reduce the rate of heat transfer by conduction, convection, and radiation. The main purpose of surface insulation is not to restrict the temperature rise, but to regulate the rate of temperature drop in order to lower the stress differences due to steep temperature gradients between the concrete surface and the interior [27-28]. This research paper, a bridge pier footing was placed with surrounding surfaces covered by formwork, then inserted by sand around the foundation. Therefore, the authors tend to study the thermal behavior of massive concrete blocks with sand-layer insulation to control the cracks at the surface of massive concrete blocks at the age of early days. The properties of the material elements used in the analysis are presented in Table 2.

Table 2. Material properties in temperature behavior analysis.

Physicalcharacteristics	Insulation (sand)	Concrete	Foundation
Thermal conduction coefficient (W/(m.°C)	0.27	2.90	1.96
Specific heat (kJ/kg.°C)	0.84	1.05	0.85
Density (kg/m^3)	1602	2400	1800
Convection coefficient (W/m^2.°C)	50	13.95	14.5
Modulus of elasticity (N/m^2)	80×10^6	3.52×10^{10}	2×10^{10}
Thermalexpansioncoefficient (1/°C)	1×10^{-5}	1×10^{-5}	1×10^{-5}
Poisson'sratio	0.2	0.2	0.2
Maximum heat of hydration of cement at 28 days (kJ/kg)	–	320	–

3. Results and Discussion

The breakdown of the concrete block and the foundation of the array on the final elements of the three – dimensional model is shown in Figure 2. With the help of the computer program Midas Civil 2017, the maximum temperature in the mass concrete with insulation thickness in differences (0–7) cm as shown in Figure 5.

Temperature distribution in the concrete mass with an insulation thickness of sand 7 cm is shown in Figure 6.

Results analysis: analyzing the results it can be noted that surface insulation by sand does not appreciably increase the maximum concrete temperature. The maximum temperature and temperature difference in the concrete with sand layers of different thickness are shown in Table 3.

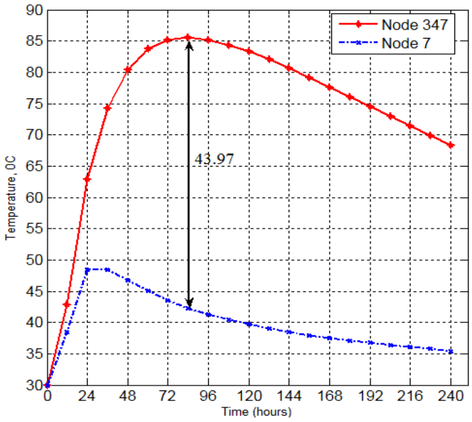

a – without the insulation layer

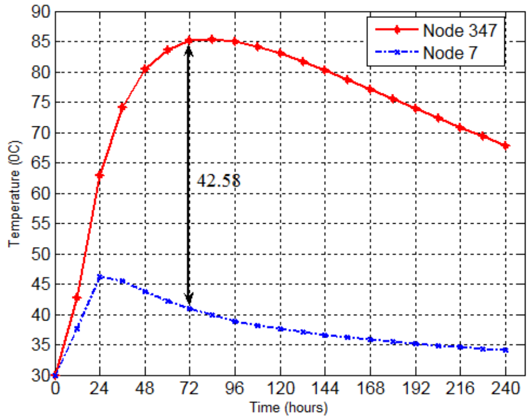

b – insulation of sand 1 cm thick layer

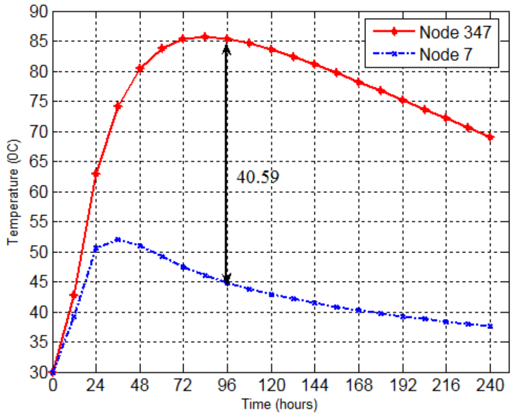

c – insulation of sand 2 cm thick layer

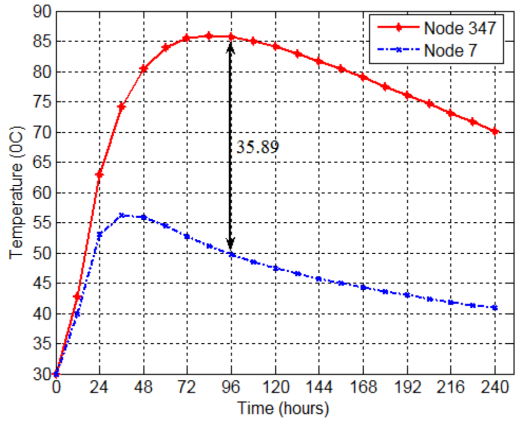

d – insulation of sand 3 cm thick layer

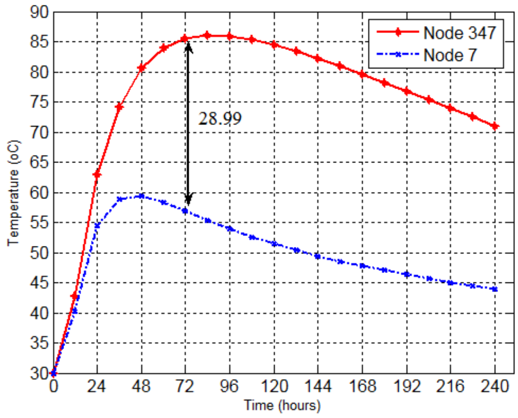

e – insulation of sand 4 cm thick layer

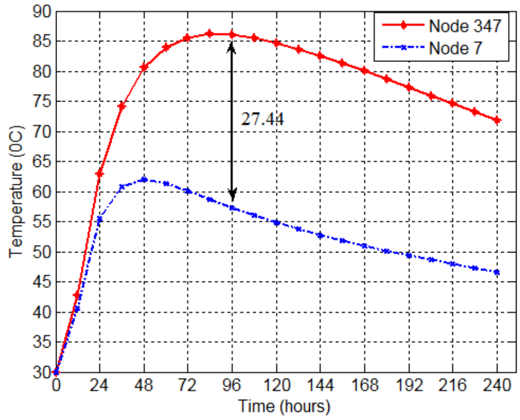

f – insulation of sand 5 cm thick layer

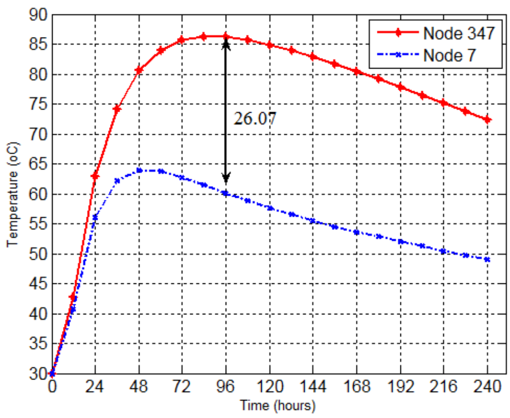

g – insulation of sand 6cm thick layer

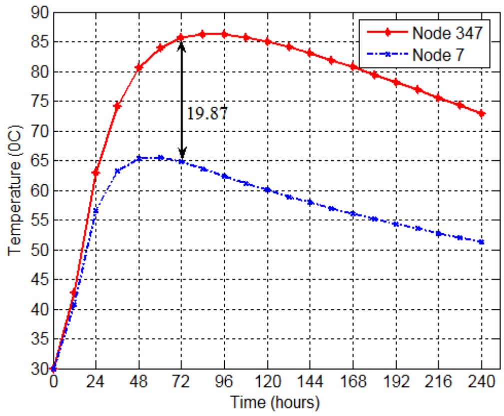

h – insulation of sand 7 cm thick layer

Figure 5. Temperature changes at the center (node 347) and at the surface (node 7) of massive concrete blocks.

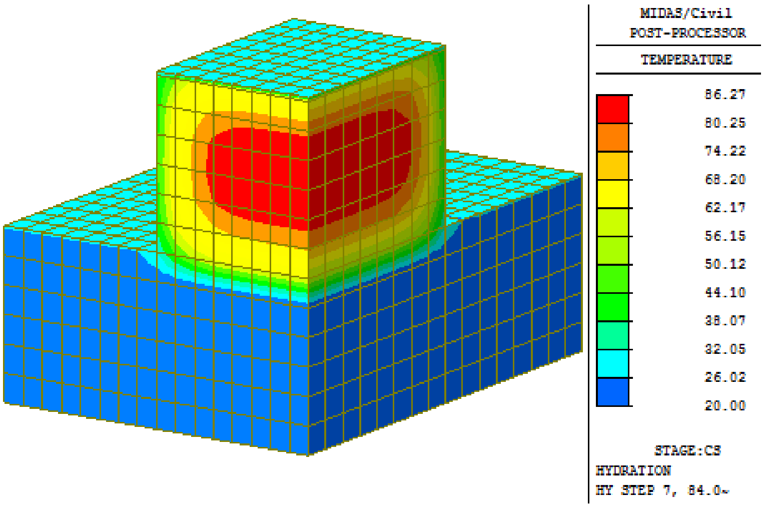

Figure 6. Temperature distribution in the concrete mass through 84 hours after laying.

Table 3. The maximum temperature and temperature difference in the concrete.

No	Insulation thickness of sand (cm)							
	0	1	2	3	4	5	6	7
Maximum temperature, °C	85.55	85.75	85.86	85.91	86.05	86.15	86.20	86.27
Temperature difference, °C	43.97	42.58	40.59	35.89	28.99	27.44	26.07	19.87

Figure 7 shows that the performance of the concrete improves as the insulation of sand thickness increases. Because when increasing the insulation thickness (0 – 7) cm, the temperature gap is reduced.

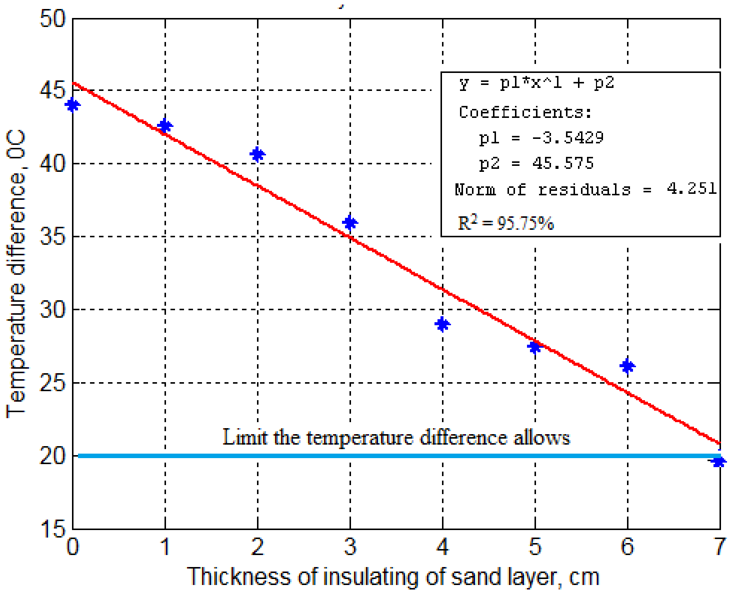

Figure 7. The relationship between the temperature difference and the thickness of the sand insulation.

Surveying range of sand thickness from 0 to 7 cm show the relation among them, and the temperature difference in the concrete mass as a function is shown in Figure 7.The correlations from the linear regressions oftemperature difference vs the thickness of the sand insulation ($y = -3.5x + 46$) R– value is R^2= 95.75 %, respectively. Therefore, it has a very good relationship.

It is worth noting that in the case of sand with a thickness of 7 cm the temperature difference between the inside and the surface not exceeds 20 °C. Besides, Figure 8 shows the stress development of the two feature points (at the center – node 347 and at the surface – node 7) with two cases: case 1 – without the insulation, case 2 – insulation of sand 7 cm in the concrete mass.

Figure 8 shows that, in the case of the concrete mass without the insulation layer, at the node 7 of the investigated mass to 168 hours of hardening the concrete, the tensile principal stress value exceeds its permissible value, leading to the formation of cracks on the surface of the concrete mass. Whereas, In the case of a concrete mass with insulation of sand 7 cm, the tensile principal stress was less than the ultimate tensile principal strength of concrete, which avoids able in forming cracks.

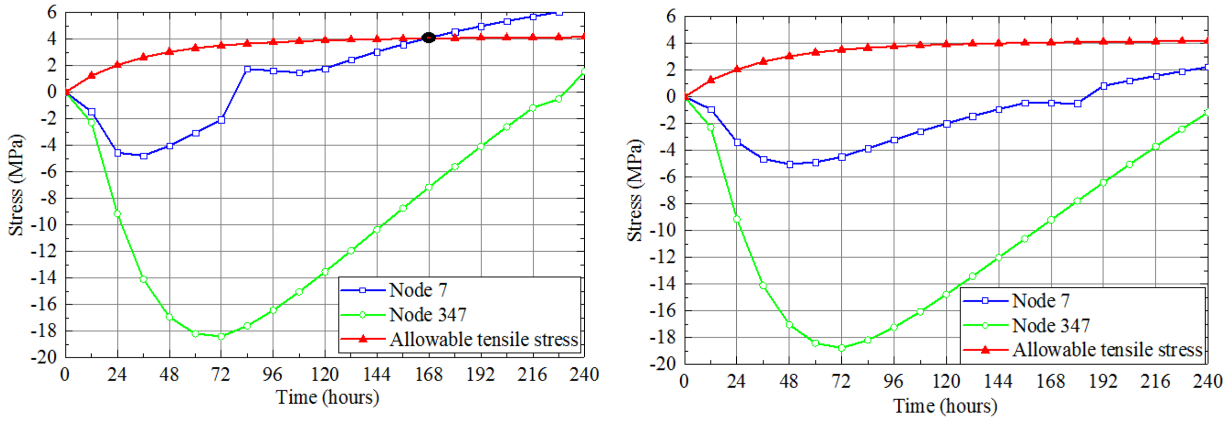

a – without the insulation layer b – insulation of sand 7 cm

Figure 8. The principal stresses development of the two points (node 347 and node 7) in the concrete mass,
a – without the insulation layer; b – insulation of sand 7 cm.

4. Conclusions

Based on the results of the study lead to the following conclusions:

1. The program Midas Civil 2017 is quite an effective tool for calculating the temperature regime and the thermal stress of concrete structures during their construction.

2. Although increasing the sand-layer insulation thickness, its effects on the maximum temperature differences between the surface and the center of the mass concrete block are not considerable.

3. The thickness of the insulation is inversely proportional to the maximum temperature difference between the center and the surface of the mass concrete. The largest temperature gap is 43.97 °C in the case without insulation sand-layer, while those gaps for (0–7) cm insulation thickness are gradual decrease. In the case of sand-layer insulation have a thickness of 7 cm –the temperature gap is 19.87 °C. In addition, the relationship between the temperature differences and the thickness of the sand insulation is given by the formula $y = -3.5x + 46$ with precision R^2= 95.75 %.

4. In case one the development of cracks may happen to the mass concrete block when the largest temperature gap is 43.97 °C and it exceeds the maximum allowable temperature difference which is 20 °C. By contrast, this phenomenon will not happen with the preservation of insulation have a thickness of 7 cm when the maximum temperature gap is lower than the limitation. As a result, this effective technique should be used to prevent cracks of the mass concrete block at an early age.

5. And future work: It is necessary to study theory in combination with the experiment to accurately evaluate the effectiveness of using insulating sand layer, avoid cracking at the face in the concrete mass at the early age. In addition, it is possible to produce sand insulation in modules. Those modules are convenient not only for construction process but also for preservation and removal process, which is applied to solve a variety of problems, such as concrete block shape, rainy and windy weather conditions.

References

1. ACI Committee 207. 207.1R-05 Guide to Mass Concrete, American Concrete Institute. 2005. Farmington Hills, Mich.
2. Tian, Y., Jin, X., Jin, N. Thermal cracking analysis of concrete with cement hydration model and equivalent age method. Computers and Concrete. 2013. Vol. 11. No. 4. Pp. 271-289. DOI: 10.12989/cac.2013.11.4.271
3. Zhang, C., Zhou, W., Ma, G., Hu, C., Li, S. A meso-scale approach to modeling thermal cracking of concrete induced by water-cooling pipes. Computers and Concrete. 2015. Vol. 15. No. 4. Pp. 485-501. DOI: 10.12989/cac.2015.15.4.485
4. Fangyuan, L., Yin, S. Full-scale test of the hydration heat and the curing method of the wet joints of a precast segmental pier of a bridge. European Journal of Environmental and Civil Engineering. 2015. Vol. 29. No. 3. Pp.348–370 [Online]. URL: https://doi.org/10.1080/19648189.2015.1119063
5. Song, S.-J., Yoo, S.-G., Park, J.-W., Kim, E.-K. A study for control of thermal cracking by heat of hydration in subway concrete box structure. Journal of the Korean Society for Railway. 2009. Vol. 12. Pp. 1024–1029.
6. Struchkova, A.Y., Barabanshchikov,Yu.G., Semenov, K.S., Shaibakova, A.A. Heat dissipation of cement and calculation of crack resistance of concrete massifs. Magazine of Civil Engineering. 2018. 78(2). Pp. 128–135. DOI: 10.18720/MCE.78.10
7. Aurich, M., Filho, A.C., Bittencourt, T.N., Shah, S.P. Finite element analysis of concrete cracking at early age. Structural Engineering and Mechanics. 2011. Vol. 37. No. 5. Pp. 459–473 [Online]. URL:https://doi.org/10.12989/sem.2011.37.5.459

8. Bushmanova, A.V., Videnkov, N.V., Semenov, K.V., Barabanshchikov, Yu.G., Dernakova, A.V., Korovina, V.K. The thermo-stressed state in massive concrete structures. Magazine of Civil Engineering. 2017. 71(3). Pp. 51–60. DOI: 10.18720/MCE.71.6
9. Bushmanova, A.V., Barabanshchikov, Yu.G., Semenov, K.V., Struchkova, A.Ya., Manovitsky, S.S. Thermal cracking resistance in massive foundation slabs in the building period. Magazine of Civil Engineering. 2017. 76(8). Pp. 193–200. DOI: 10.18720/MCE.76.17
10. Zhang, X., Li, S., Li, Y., Ge, Y., Li, H. Effect of superficial insulation on roller-compacted concrete dams in cold regions.Advances in Engineering Software. 2018. Vol. 42. No. 11. Pp. 939–943. DOI:10.1016/j.advengsoft.2011.06.004
11. Tu, D.A., Adrian, M.L., Mang, T., Anh, P.N. Importance of insulation at the bottom of mass concrete placed on soil with high groundwater. Transportation Research Record Journal of the Transportation Research Board. 2013. Vol. 2342. No. 1. Pp. 113–120.
12. Bamforth P.B. Early-age thermal crack control in concreter. 2017. London.
13. Lam, T.V., Chuc, N.T., Boris, B., Michael, J.B. Composition and early-age temperature regime in a massive concrete foundation. 2018. MATEC Web of Confer. Vol.196. 8p. [Online]. URL: https://doi.org/10.1051/matecconf/201819604017
14. Patil, A. Heat of hydration in the placement of mass concrete. International Journal of Engineering and Advanced Technology (IJEAT). 2015. Vol. 4. No. 3. 4p.
15. Lee, M.H., Chae, Y.S., Khil, B.S., Yun, H.D. Influence of casting temperature on the heat of hydration in mass concrete foundation with ternary cement. Applied Mechanics and Materials. 2014. Vol. 525. Pp. 478-481. DOI: 10.4028/www.scientific.net/AMM.525.478
16. Li, B., Wang, Z., Jiang, Y., Zhu, Z. Temperature control and crack prevention during construction in steep slope dams and stilling basins in high-altitude areas. Advances in Mechanical Engineering. 2018. Vol. 10. No. 1. 15p. DOI: 10.1177/1687814017752480
17. Klemczak, B., Knoppik-Wrobel, A. Early age thermal and shrinkage cracks in concrete structures-Description of the problem. Architecture Civil Engineering Environment. 2011.Vol. 3. Pp. 55–70.
18. Van Lam, T., Nguyen, C.C., Bulgakov, B.I., Anh, P.N Composition calculation and cracking estimation of concrete at early ages. Magazine of Civil Engineering. 2018. 82(6). Pp. 136–148. DOI: 10.18720/MCE.82.13
19. Akin, J.E. Finite element for analysis and design. Texas, USA. 1994. 548p.
20. Abeka, H., Agyeman, S., Adom-asamoah, M., Hussain, R.R. Thermal effect of mass concrete structures in the tropics: experimental, modellingand parametric studies. Journal Cogent Engineering. 2017. Vol. 4. No. 1. Pp. 185–192.
21. Zhu, B. Thermal stresses and temperature control of mass concrete. Published by Elsevier Inc. 2014. 497p.
22. ACI 209.2R-08. Guide for modeling and calculating shrinkage and creep in hardened concrete. AmericanConcreteInstitute. 2008. 48p.
23. SP 357.1325800.2017. Konstruktsii betonnyye gidrotekhnicheskikh sooruzheniy [Concrete constructions hydraulic structures. Rules of production and acceptance of work].
24. Noorzaei, J., Bayagoob, K.H., Thanoon, W.A., Jaafar, M.S. Thermal and stress analysis of kintarcc dam. Journal Engineering Structures. 2006.No. 28. Pp. 1795–1802.
25. ACI 318-2005. Building Code Requirements for Structural Concrete. American Concrete Institute, Farmington Hills, Mich. 2005. 31 p.
26. Khoa, H.N, Cong, V.C. Analyzing temperature field and thermal stress in massive concrete by finite element method. Journal of Science and Technology building. 2012. No. 14(12). Pp. 17–27.
27. Chuc, N.T., Lam, T.V., Bulgakov, B.I. Designing the composition of concrete with mineral additives and assessment of the possibility of cracking in cement-concrete pavement. Materials Science Forum. 2018. Vol. 931. Pp. 667–673[Online]. URL: https://doi.org/10.4028/www.scientific.net/MSF.931.667
28. Korotchenko, I.A., Ivanov, E.N., Manovitsky, S.S., Borisova, V.A., Semenov, K.V., Barabanshchikov,Yu.G. Deformation of concrete creep in the thermal stress state calculation of massive concrete and reinforced concrete structures Magazine of Civil Engineering. 2017. 69(1). Pp. 56–63. DOI: 10.18720/MCE.69.5

Contacts:

Trong Chuc Nguyen, +7(966)3319199; ntchuc.mta198@gmail.com
Xuan Bach Luu, +84979940455; xuanbachmta@gmail.com